Analytical study of the effect of the geometrical parameters during the interaction of regular wave-horizontal plate-current

Smail Naasse[1], Meriem Errifaiy[1]*, Chakib Chahine[1]

[1] Laboratory Physics of Polymers and Critical Phenomena, Hassan Ⅱ University Casablanca, Casablanca P B 7955, Morocco

Abstract

The present work is an analytical study of the influence of geometrical parameters, such as length, thickness and immersion of the plate, on the reflection coefficient of a regular wave for an immersed horizontal plate in the presence of a uniform current with the same direction as the propagation of the incident regular wave. This study was performed using the linearized potential theory with the evanescent modes while searching for complex roots to the dispersion equation that are neither pure real nor pure imaginary. The results show that the effects of the immersion and the relative length on the reflection coefficient of the plate are accentuated by the presence of the current, whereas the plate thickness practically does not have an effect if it is relatively small.

Key words: current, regular wave, evanescent modes, reflection, dispersion equation, complex roots, geometrical parameters

---

1 Introduction

A submerged horizontal plate may serve as breakwater to protect harbors, inlets and beaches from wave action. As with all submerged structures, the horizontal plate does not obstruct the ocean view, which is critical for recreational and residential shore development. Moreover, the horizontal plate enables the circulation of water above and beneath it; hence, its environmental impact is minimal.

With the plate being a more or less thick rectangular structure, the parameters that come into play when interacting with regular waves are the characteristics of the incident wave, the geometry of the plate (length, thickness), its nature (porosity, elasticity), its disposition (vertical, inclined or horizontal) and its immersion. Several researchers are particularly interested in the effect of the geometrical parameters during the interaction of regular waves with a submerged plate. Patarapanich (add the reference) showed analytically, using the wave plane model, that the reflection coefficient depends on the relative depth of the incident wave, the immersion ratio of the plate and the length of the plate relatively to the wavelength of the wave that propagates above the plate (Patarapanich, 1984) and compared experimental results with the solution obtained numerically by the finite-element method (Patarapanich and Cheong, 1989). The interaction of a rectangular structure with a regular wave was studied analytically by Zheng et al. (2007a, b), notably focusing on the effect of the thickness, the immersion and the length of the structure on the reflection coefficient, the hydrodynamic coefficients and the forces exerted by the regular waves on the structure. The interaction of regular waves with a thick plate in the presence of a permeable breakwater was numerically investigated by Hsu and Wu (1998) and Rao et al. (2009), they experimentally studied the effect of the relative depth. The case of a porous plate was investig-

ated numerically (BEM) by Yueh and Chuang (2009). In 2014, Behera and Sahoo (2015) investigated the interaction of a gravity wave with a flexible porous plate. An experimental study on the attenuation of regular waves by an inclined plate was presented by Acanal et al. (2013). In 2014, Ning et al. (2014) presented a numerical study on the higher harmonics during the interaction of a nonlinear wave with a horizontal cylinder in the presence of a current. In 2017, Bai et al. (2017) investigated the forces exerted on a horizontal cylinder during the passage of a regular wave in the presence of a sheared current. However, in these studies, the effects of geometrical parameters on wave reflection by a submerged plate in the presence of a current were not investigated.

In this work, we are interested in the effects of the geometrical parameters of a rigid and impermeable horizontal plate on the reflection coefficient of regular waves propagating in the presence of a uniform current having the same direction as the incident wave. This study was conducted as part of the linear potential theory using the model of evanescent modes. The roots of the dispersion equation are searched as complex numbers to obtain solutions with real nonzero and imaginary nonzero parts (Errifaiy et al., 2016).

First, we present the formulation of the problem of the interaction of a regular wave with a horizontal plate in the presence of a current. The velocity potential sought is in the form of a superposition of the potential corresponding to the current and that corresponding to a regular wave. The velocity potential in the subdomains upstream and above the plate is the sum of the uniform current, two modes propagating in opposite directions and a series of evanescent modes. In the subdomain downstream of the plate, the velocity potential is the sum of the uniform current, a mode propagating downstream and a series of evanescent modes. In the subdomain below the plate, the velocity potential

*Corresponding author, E-mail: errifaiy.m@gmail.com

is the sum of the uniform current, an oscillating horizontal current and a series of evanescent modes. By means of the matching conditions between the subdomains that express the continuity of the velocity potential and of the horizontal velocity at the attack and trailing edges of the plate, one obtains a linear algebraic system whose unknowns are the constants involved in the writing of the potential. The resolution of this system allows us to determine the reflection coefficient.

Second, we studied the effect of the geometric parameters on the reflection of a regular wave by a submerged horizontal plate in the absence of a current: the results concerning the effect of the immersion ratio and the plate length during the interaction of wave-thin plate are compared of those of Patarapanich and Cheong (1989) and of those of Brossard et al. (2009). The results concerning reflection by a thick plate are compared with those of Liu and Iskandarani (1991).

Afterward, we studied the effect of geometric parameters on the reflection of a regular wave by a submerged horizontal plate in the presence of a current: the results are compared with those of Rey and Touboul (2011) and with those of Lin et al. (2014). In these two cases, the reflection coefficient is calculated using the present model in two ways: first by supposing that the plate thickness is zero and second by taking into account the real plate thickness.

Finally, the model is used to predict the effects of the relative plate thickness, the immersion ratio and the relative plate length on the reflection coefficient. Notably, we investigated the effect on the maximum of the reflection coefficient and on the reflection bandwidth. The reflection band is defined by adopting the criterion used in electronics to define the pass band. With this definition, the width of the reflection band is the width of the interval $[k_1H, k_2H]$ so that the value of the reflection coefficient corresponding to k_1H and k_2H is equal to $R_{\max}/\sqrt{2}$, where $R_{\max}$ denotes the maximum of the reflection coefficient.

2 Interaction of wave-current-plate

In this part, we present the calculation of the reflection coefficient of a regular wave in the presence of a uniform current interacting with a fixed horizontal plate completely immersed in a channel. This study was conducted as part of the linearized potential theory using the evanescent modes model. The studied regular wave is of low wave steepness, and the surface tension is negligible. A monochromatic wave is emitted upstream; downstream, the wave does not undergo any reflection.

2.1 *Velocity potential*

The horizontal plate is totally immersed in a channel. The plate is e in thickness and $2l$ in length, covering the entire width of the channel. The domain of study is reported as a Cartesian coordinate system (O, x, y), in which the axis (Oy) is directed vertically upward, the axis (Ox) coincides with the position of the free surface at rest, and origin O coincides with the center of the plate orthogonal projection on the axis (Ox). The geometry of the domain of study leads us to define four subdomains, as shown in Fig. 1.

Seeking the potential in the form of a superposition of the potentials associated with the current $\phi_c(x, y, t) = Ux$ and with a monochromatic regular wave $\phi_h(x, y, t) = \varphi(x, y)\,e^{i\omega t}$, (Rey et al., 2003; Errifaiy et al., 2016) obtained the total potential as follows:

In subdomains D_p, $1 \leqslant p \leqslant 3$:

$$\phi_p(x, y, t) = Ux + \Big[A_p e^{ik_p^- x}\cosh\big(k_p^-\,(y+ H_p)\big) + B_p e^{ik_p^+ x}\cosh\big(k_p^+\,(y + H_p)\big) + \sum_{n=1}^{N} A_{pn}e^{k_{pn}x}\cos\big(k_{pn}\,(y + H_p)\big) + B_{pn}e^{-k_{pn}x}\cos\big(k_{pn}\,(y + H_p)\big)\Big]e^{i\omega t}. \tag{1}$$

In this equation, H_1 and H_2 are both equal to the water depth in the channel $(H_1=H_2=H)$, H_3 is equal to the plate immersion $(H_3=h)$, ω is the wave pulsation, N denotes the number of evanescent modes, A_{1n} and B_{2n} are all zero, A_1 is given by $A_1 = ga_i\,\dfrac{1}{\big(\omega - Uk_1^-\big)\cosh\big(k_1^- H\big)}$ (where a_i is the amplitude of the wave that propagates at the free surface and g is the acceleration of gravity), and the constants $k_p^{\pm}$ and k_{pn} are the roots of the following equations:

$$\big(\omega \pm U\big(k_p^{\pm}\big)\big)^2 = g\big(k_p^{\pm}\big) \times \tanh\big(\big(k_p^{\pm}\big)H_p\big), \tag{2}$$

$$\big(i\omega + U(k_{pn})\big)^2 = g(k_{pn}) \times \tan\big((k_{pn})H_p\big). \tag{3}$$

In subdomain D_4:

$$\phi_4(x, y, t) = Ux + \Big[\Big(A_4 + B_4x + \sum_{n=1}^{N}\big(A_{4n}e^{-(\mu_n x)} + B_{4n}e^{(\mu_n x)}\big)\cos\big(\mu_n\,(y + H)\big)\Big)\Big]e^{i\omega t}. \tag{4}$$
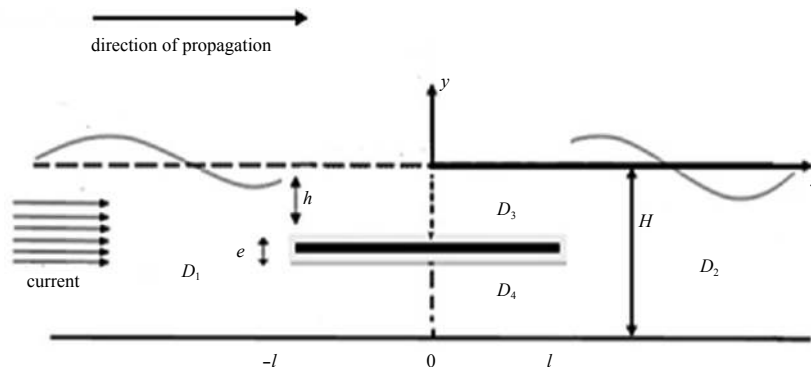

Fig. 1. Descriptive schemas of the wave propagation with a submerged plate in the presence of a current.

$$\mu_n = \frac{n\pi}{H - h - e}, \tag{5}$$

where e is the plate thickness.

All constants $\{B_1, B_{1n}, A_3, B_3, A_{3n}, B_{3n}, A_4, B_4, A_{4n}, B_{4n}, A_2$ and A_{2n} for $1 \leqslant n \leqslant N\}$ that are present in Eqs (1) and (4) are unknown.

The roots of Eq. (2) are the wavenumbers of the propagating modes. The roots of Eq. (3) correspond to evanescent modes. In the absence of a current ($U=0$), these roots are pure real. However, in the presence of a current, it is easy to verify, first, that this equation has no pure real roots and, second, that the pure imaginary roots are those corresponding to Eq. (2). Therefore, to establish this model, it is necessary to search for roots (k_{pn}) with a nonzero real part and a nonzero imaginary part as well.

Equation (1) shows that the velocity potential corresponding to subdomains D_1 and D_3 is the sum of the uniform current, two modes propagating in opposite directions and a series of evanescent modes. In subdomain D_2, the velocity potential is the sum of the uniform current, a mode propagating downstream and a series of evanescent modes. Equation 4 shows that the velocity potential corresponding to subdomain D_4 is the sum of the uniform current, an oscillatory current and a series of evanescent modes.

2.2 *Reflection coefficient calculation*

The reflection coefficient of the regular wave that propagates at the free surface is given by

$$R = \frac{(\omega + Uk_1^+)}{(\omega - Uk_1^-)} \times \frac{\cosh(k_1^+ H)}{\cosh(k_1^- H)} \times \frac{B_1}{A_1}. \tag{6}$$

To determine the reflection coefficient R, we must resolve a linear algebraic system of ($6N+6$) equations and ($6N+6$) unknowns, which are the constants $\{B_1, B_{1n}, A_3, B_3, A_{3n}, B_{3n}, A_4, B_4, A_{4n}, B_{4n}, A_2$ and A_{2n} for $1 \leqslant n \leqslant N\}$ that are present in Eqs (A1) and (A4) (see Appendix).

This system is obtained by means of the matching conditions between the subdomains that express the continuity of the velocity potential and of the horizontal velocity at the attack and trailing edges of the plate ($x=-l$ and $x=l$, respectively).

The elements of the matrix corresponding to this system depend on the following: the relative depth kH (which expresses the ratio of the water depth in the channel to the wavelength of the incident wave in the absence of a current), the Froud number

$U/\sqrt{gH}$ and the geometrical parameters, namely, the plate immersion ratio (h/H), the relative plate length ($2l/h$) and the relative plate thickness (e/h) (see Appendix). Accordingly, the reflection coefficient depends on the same parameters.

3 Effects of the geometrical parametrical parameters in the absence of a current

3.1 *Immersion ratio and relative plate length effect*

During the interaction of a regular wave with a horizontal plate immersed in the absence of a current, the effects of immersion and plate length were experimentally and numerically (finite element method) studied by Patarapanich and Cheong (1989) and experimentally studied by Brossard et al. (2009). We compared the values of the reflection coefficient calculated using the present model with the results of Patarapanich (Fig. 2) and with those of Brossard et al. (2009) (Fig. 3). In these figures, the coefficient of reflection is represented as a function of the ratio of the plate length ($2l$) to the wavelength (L) of the wave propagating above the plate.

The results of the model fit well with the results calculated via the finite element method by Patarapanich (Fig. 2) and are close to the experimental results of Patarapanich (Fig. 2) and those of Brossard (Fig. 3).

The curves in Figs 2 and 3 show the following:

(1) The reflection coefficient increases as the immersion ratio decreases.

(2) At a constant immersion ratio, the reflection coefficient increases to the maximum and then decreases.

3.2 *Plate thickness effect*

In the available literature, most studies assumed the plate thickness to be zero for simplicity. The plate thickness was considered only in a few studies.

Liu and Iskandarani (1991) studied the interaction of a linear and nonlinear wave with a thick plate.

Liu et al. (2009) by studying the reflection coefficient evolution as function of the plate length to wavelength ratio during the interaction of water waves with twin plates, showed that the reflection coefficient decreases with increasing plate thickness.

Zheng et al., (2007b) studied the interaction between water waves and a rectangular structure for an oblique incidence. In their study, the representation of the reflection coefficient as a function of kH showed that the reflection coefficient increases with the increase of the structure thickness.
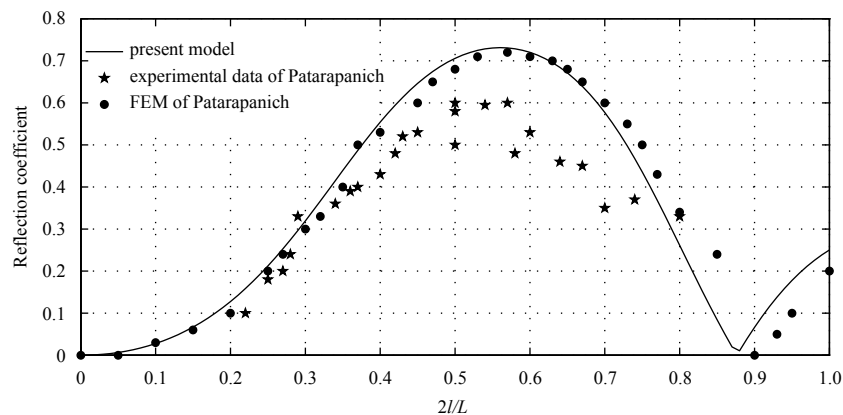

Fig. 2. Reflection coefficient as a function of $2l/L$ for a relative depth $kH=1.256$ and a plate immersion ratio $h/H=0.3$.
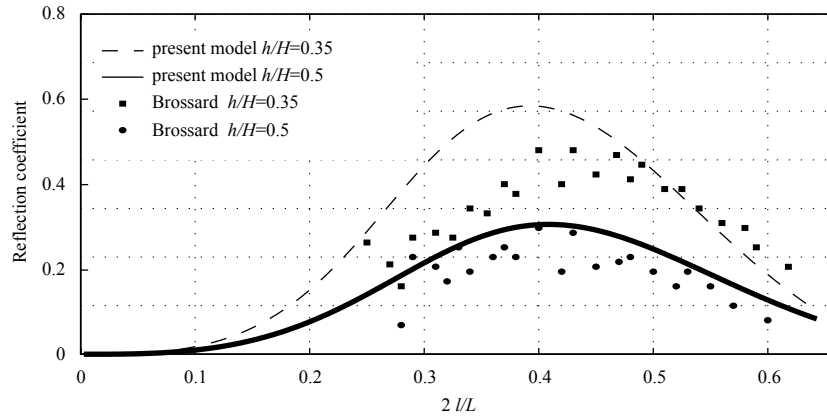
Fig. 3. Reflection coefficient as a function of $2l/L$ for a plate length $2l$=25 cm and two values of the plate immersion ratio h/H=0.5, 0.35.

To study the effect of the plate thickness on the reflection coefficient during the interaction of a regular wave with a thick plate, we first compared the results calculated using this model with those of Liu and Iskandarani (1991). The results presented in Fig. 4 are in good agreement with those of Philip L-F Liu and Iskandarani (1991). Second, we calculated the reflection coefficient of a regular wave, in normal incidence, during its interaction with a rectangular structure. In keeping the settings of the configuration taken by Zheng et al. (2007b) (except for the incidence angle), we represent the reflection coefficient versus kH in Fig. 5. The curves obtained are similar to those of Zheng et al. (2007b).

4 Effect of the geometrical parameters in the presence of a current

As shown above, during the regular wave–current–plate interaction, in addition to the current velocity, the reflection coefficient of a regular wave also depends on the geometrical parameters of the examined problem. These geometrical parameters are the relative depth of water in the channel, the relative thickness of the plate, its immersion ratio and its relative length. The present model is used to study the effect of each of these parameters on the reflection coefficient. This study was conducted as part of the linearized potential flow theory using the evanescent modes model. To take account of the evanescent modes in the presence of a current, the dispersion equation was solved by seeking complex roots that are neither pure real nor pure imaginary. In this model, the number of evanescent modes taken into account is N=30 (Errifaiy et al., 2016).
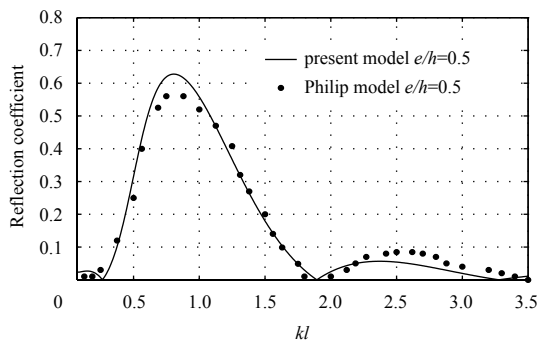

Fig. 4. Reflection coefficient as a function of kl for l/h=2, relative plate thickness e/h=0.5 and a plate immersion ratio h/H=0.25.
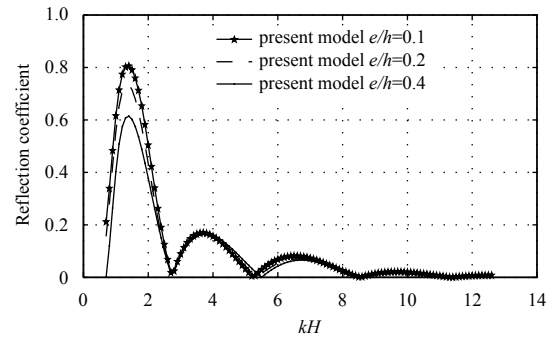

Fig. 5. Reflection coefficient as a function of kH for a plate immersion ratio h/H=0.2, a relative plate length $2l/h = 6$, and different values of the relative plate thickness e/h=0.1, 0.2, 0.4.

4.1 *Plate thickness effect*

To study the effect of the plate thickness, the reflection coefficient is calculated using this model with a thin plate and a thick plate in the presence of a current. First, the results were compared with those obtained experimentally by Rey and Touboul (2011) and with the numerical results of Lin et al. (2014). Afterward, the model was used to predict the effect of the relative plate thickness (e/h) on the reflection coefficient for different values of the plate immersion ratio (h/H).

4.1.1 *Comparison with the data of Rey and Touboul (2011)*

Rey and Touboul (2011) experimentally investigated the reflection of a regular wave in the presence of a current of velocity (U=0.3 m/s), interacting with a plate of thickness e=0.1 m immersed in a flat horizontal channel with a water depth H=3 m. The plate is immersed at depth h=0.5 m below the level of the free surface.

We compare our results with those of Rey and Touboul (2011) in Fig. 6. The calculations of the reflection coefficient by the present model were performed, first, by keeping the value of the thickness taken by these authors and, second, by supposing that the plate is without thickness.

In Fig. 6, we represent the dependence on the period of the values of the reflection coefficient measured experimentally by Rey and Touboul (2011) and calculated analytically by the present model. The analytical calculations were made in the presence of a current velocity (U=0.3 m/s), for a thin plate (e=0 m) and a plate of thickness (e=0.1 m).
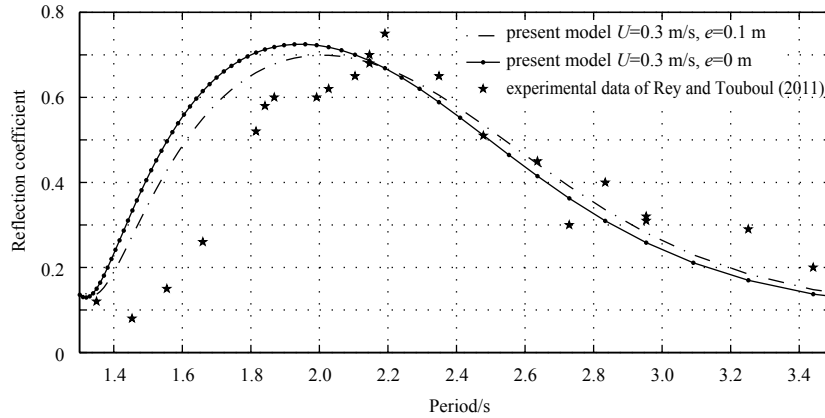
Fig. 6. Reflection coefficient as a function of the period for plate thicknesses e=0.1 m and e=0 m, plate length $2l$=1.53 m, plate immersion h=0.5 m, water depth H=3 m and current velocity U=0.3 m/s.

The curves in Fig. 6 show the following:

(1) The difference between the analytical results calculated by the present model for e=0 m and e=0.1 m is weak.

(2) There is good agreement between the results of Rey and those of the model, especially for the long periods (the long waves). The shift in the range of the short periods (short wavelengths) may be explained by the fact that the analytical model does not take into account the vortex emission by the plate (Lebon et al., 2016) or the surface tension, whose effect increases when the wavelength decreases.

4.1.2 *Comparison with the computation of Lin et al. (2014)*

Lin et al. (2014) performed a numerical study (BEM) of the same problem with a plate of thickness e=0.01 m immersed at h=0.1 m and h=0.07 m with a water depth H=0.2 m for U/C_{g0} =0.12 (ratio of the current velocity relative to the C_{g0} group velocity calculated in the absence of a current).

We compare our results with those of Lin et al. (2014) in Fig. 7. The calculations of the reflection coefficient by the present model were first performed by keeping the value of the thickness taken by these authors and then by supposing that the plate is without thickness.

In Fig. 7, we represent the dependence on the period of the values of the reflection coefficient for $U/C_{g0} = 0.12$ (ratio of the current velocity relative to the C_{g0} group velocity calculated in the absence of a current). The results calculated by this model with a thin plate (e=0 m) and a thick plate (e=0.01 m) are compared with those calculated numerically by Lin et al. (2014).

The curves in Fig. 7 show that there is good agreement between the result calculated by this model with plate thicknesses e=0 m and e=0.01 m and those calculated numerically by Lin et al. (2014).

4.1.3 *Model prediction*

The results in Figs 6 and 7 show the following:

(1) The results calculated by the present model are in agreement with the experimental values of Rey and Touboul (2011) (Fig. 6) and the values of Lin et al. (2014) (Fig. 7).

(2) The difference between the results calculated by this model with a plate without thickness and those calculated taking into account the thickness of the plate is weak.

In the following, we used the model to study the variation of the reflection coefficient for different thicknesses of the plate at different immersions.

Figures 8a–d represent the values of the reflection coefficient as a function of kH (relative depth of the incident wave in the absence of a current) for different values of the relative plate thickness (e/h), different values of the plate immersion ratio (h/H) and Froud number $U/\sqrt{gH} = 0.045$. It shows that reflection coefficient decreases when the relative plate thickness (e/h) increases.

In Table 1, we present the relative difference in the maximum of the reflection coefficient $(M–M_0)/M_0$, where M_0 is the reflection coefficient maximum for the plate without thickness (e=0 m).
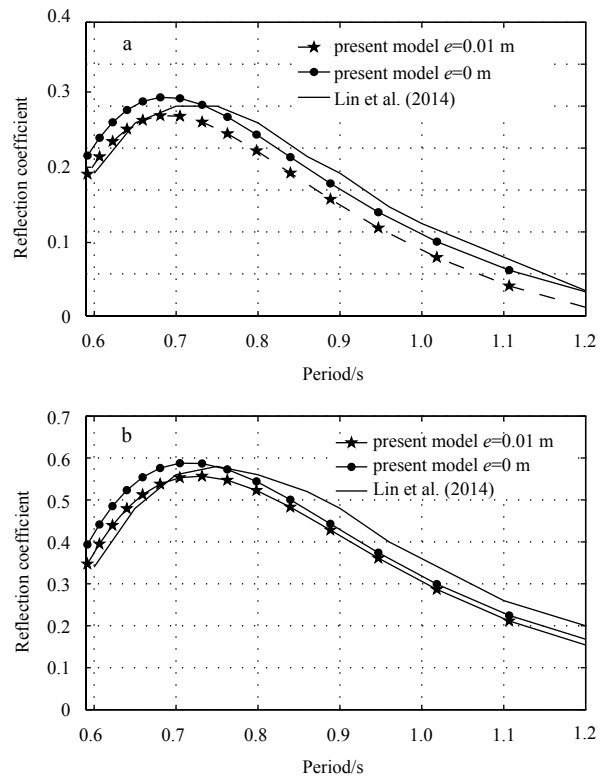

Fig. 7. Reflection coefficient as a function of period for a plate length $2l$=0.25 m, water depth H=0.2 m, relative current velocity $U/C_{g0} = 0.12$ (C_{g0} is the group velocity at T=0.75 s) and plate thicknesses e=0 m and e=0.01 m. In Fig. 7a, the plate immersion h= 0.1 m, and in Fig. 7b, h=0.07 m.
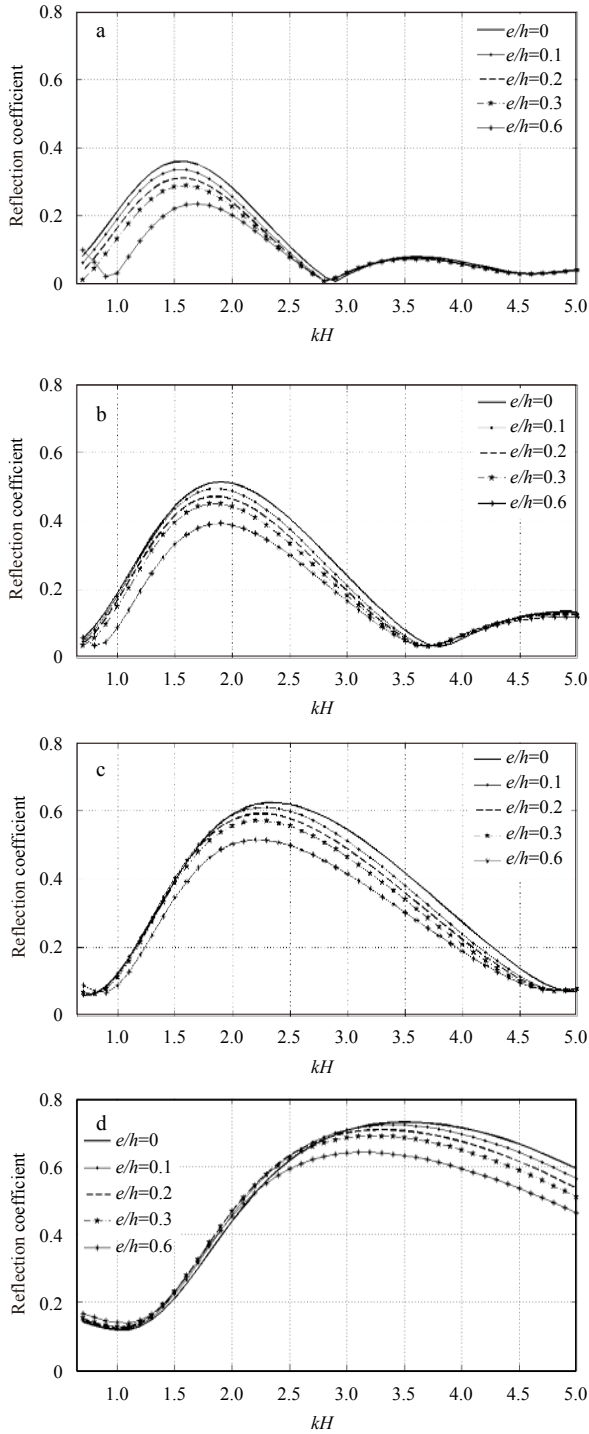
Fig. 8. Reflection coefficient as a function of *kH* for a relative plate length 2*l*/*h*=3, Froud number $U/\sqrt{gH}$=0.045, and different values of relative plate thickness *e*/*h*=0, 0.1, 0.2, 0.3 and 0.6. *a*. Immersion ratio *h*/*H*=0.5, b. *h*/*H*=0.35, *c*. *h*/*H*=0.25, and d. *h*/*H*=0.15.

At the same immersion, the relative difference in the maximum of the reflection coefficient $(M-M_0)/M_0$ increases when the relative thickness increases. For the same relative thickness, the relative difference in the maximum of the reflection coefficient $(M-M_0)/M_0$ decreases when the immersion ratio decreases. For relative thickness (e/h) =0.1, the relative difference in the maximum of the reflection coefficient $(M-M_0)/M_0$ is approximately 7%

for immersion 0.5 and does not exceed 3% for other immersions.

Consequently, we can conclude that the relative plate thickness effect on the reflection coefficient decreases when the immersion ratio decreases.

4.2 *Effect of plate immersion*

In this section, we study the effect of the plate immersion ratio on the reflection coefficient during the regular wave–current–thin plate interaction. For this study, the reflection coefficient calculated by the present model is represented as a function of *kH* (relative depth of the incident wave in the absence of a current) for different values of the plate immersion and different values of the Froude number.

We study the effect on the maximum of the reflection coefficient and on the reflection bandwidth. The reflection band is defined by adopting the criterion used in electronics to define the pass band. With this definition, the width of the reflection band is the width of the interval $[k_1H, k_2H]$ so that the value of the reflection coefficient corresponding to k_1H and k_2H is equal to $R_{\max}/\sqrt{2}$, where $R_{\max}$ denotes the maximum of the reflection coefficient.

To study the effect of the plate immersion ratio, we represent the variations of the reflection coefficient as a function of the relative depth *kH* for different immersion ratios (*h*/*H*=0.25, *h*/*H*=0.50, *h*/*H*=0.75) (Fig. 9). The analytical calculations were performed using this theoretical model for a relative plate length (2*l*/*h*)=3. Three cases are considered: in the absence of a current (Fig. 9a) and for two values of the Froud number $U/\sqrt{gH}$ =0.045 (Fig. 9b) and $U/\sqrt{gH}$ =0.061 (Fig. 9c). In Table 2, we presented the reflection bandwidth and the relative difference of the maximum of the reflection coefficient $(M-M_0)/M_0$, where M_0 is the reflection coefficient maximum in the absence of a current.

The curves in Figs 9a–c and the results presented in Table 2 show that:

(1) The reflection coefficient maximum and the width of the reflection band decrease with the increase of the plate immersion ratio.

(2) When the plate immersion ratio increases, the width of the reflection band is shifted to higher values of *kH* (short wavelength).

(3) When the Froud number increases, the reflection coefficient maximum also increases, the reflection band is not shifted and its width is practically unchanged.

Thus, we can conclude that the nearer the plate is to the free surface (low immersion), the more important is the effect of current and the shift of the efficiency of the plate toward the large values of *kH*.

4.3 *Effect of the relative plate length*

To consider the impact of the length of the plate on the reflection coefficient in the presence of a current, we represent the variations of the reflection coefficient as a function of *kH* (relative depth of the incident wave in the absence of a current) for different values of the relative length of the plate (2*l*/*h*=3, 3.5 and 4) and for different values of the Froud number. The three cases considered are $U/\sqrt{gH} = 0$ (in the absence of a current) (Fig. 10a), $U/\sqrt{gH} = 0.045$ (Fig. 10b) and $U/\sqrt{gH} = 0.061$ (Fig. 10c). In Table 3, we present the reflection bandwidth and the relative difference of the maximum reflection coefficient $(M-M_0)/M_0$, where M_0 is the reflection coefficient maximum in the absence of a current.

The curves in Figs 10a–c and the results presented in Table 3

Table 1. Relative difference in the maximum value of the reflection coefficient for Froud number $U/\sqrt{gH} = 0.045$

e/h	$h/H=0.5$				$h/H=0.35$				$h/H=0.25$				$h/H=0.15$			
	0.1	0.2	0.3	0.6	0.1	0.2	0.3	0.6	0.1	0.2	0.3	0.6	0.1	0.2	0.3	0.6
$\dfrac{M - M_0}{M_0}$	0.07	0.14	0.20	0.35	0.03	0.08	0.12	0.23	0.02	0.05	0.08	0.17	0.01	0.03	0.06	0.12
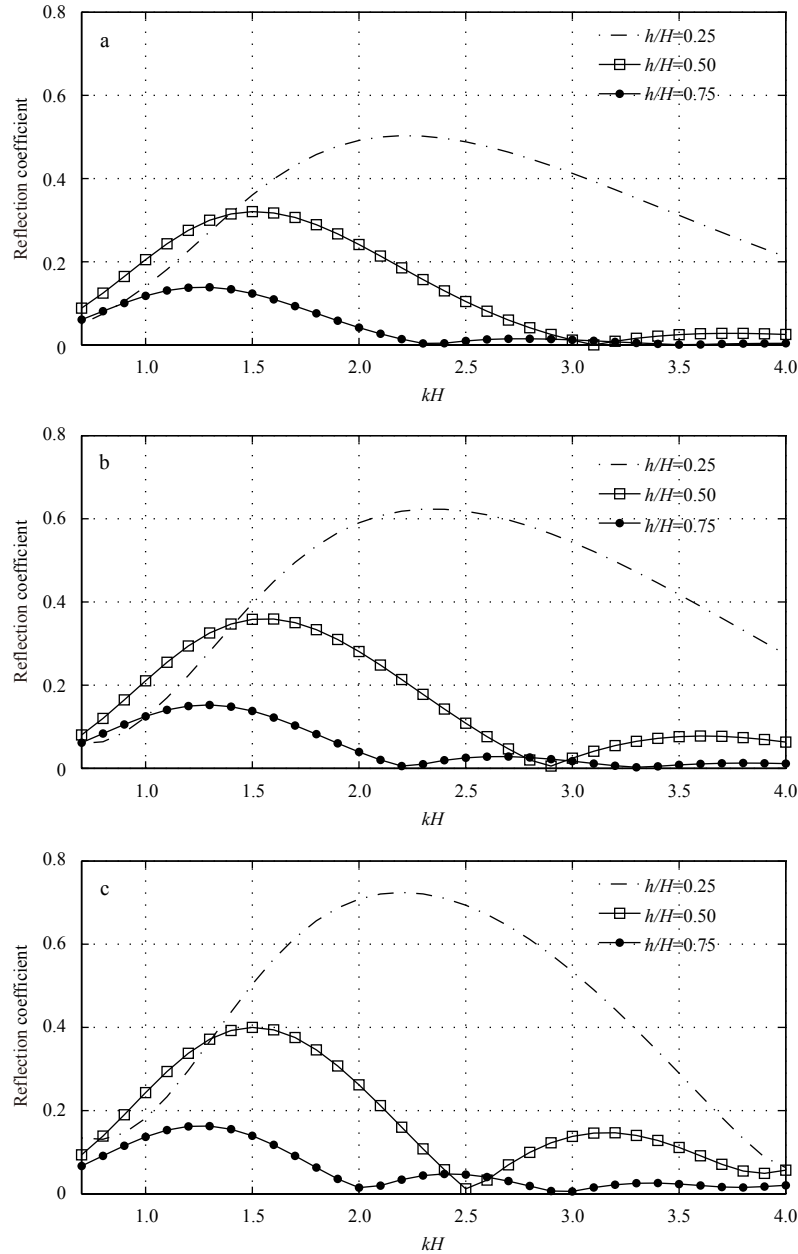
Fig. 9. Reflection coefficient as a function of *kH* for a thin plate (*e*=0 m), a relative plate length 2*l*/*h*=3, and different values of the plate immersion ratio (*h/H*=0.25, 0.50 and 0.75). a. Froud number $U/\sqrt{gH} = 0$, b. $U/\sqrt{gH} = 0.045$, and c. $U/\sqrt{gH} = 0.061$.

show that:

(1) The reflection coefficient maximum increases very slightly with the increase of the relative plate length.

(2) When the relative plate length increases, the reflection band is shifted to low values of *kH* (high wavelength) and the width of this band decreases.

(3) When the Froud number increases, the reflection coefficient maximum increases and the reflection band is not shifted and is of practically unchanged width.

We concluded that the effect of the relative length of the plate on the reflection coefficient is accentuated by the current velocity and that this accentuation decreases with the increase of the relative plate length.

5 Conclusions

In this paper, we studied the influence of the geometrical parameters of a plate during the regular wave–current–plate interaction. These parameters are the relative depth of water in the

Table 2. Relative difference in the maximum value of the reflection coefficient and the reflection bandwidth for different values of the immersion ratio (h/H=0.25, 0.50 and 0.75) and different values of the Froud number ($U/\sqrt{gH}$=0, 0.045 and 0.061)

h/H	$\dfrac{U}{\sqrt{gH}} = 0$			$\dfrac{U}{\sqrt{gH}} = 0.045$			$\dfrac{U}{\sqrt{gH}} = 0.061$		
	0.25	0.50	0.75	0.25	0.50	0.75	0.25	0.50	0.75
$\left\lvert \dfrac{M - M_0}{M_0} \right\rvert$				23.7%	12%	10%	43.5%	24.8%	17.5%
$\lvert k_2H - k_1H \rvert$	1.80	1.05	0.85	1.80	1.00	0.80	1.60	0.85	0.70
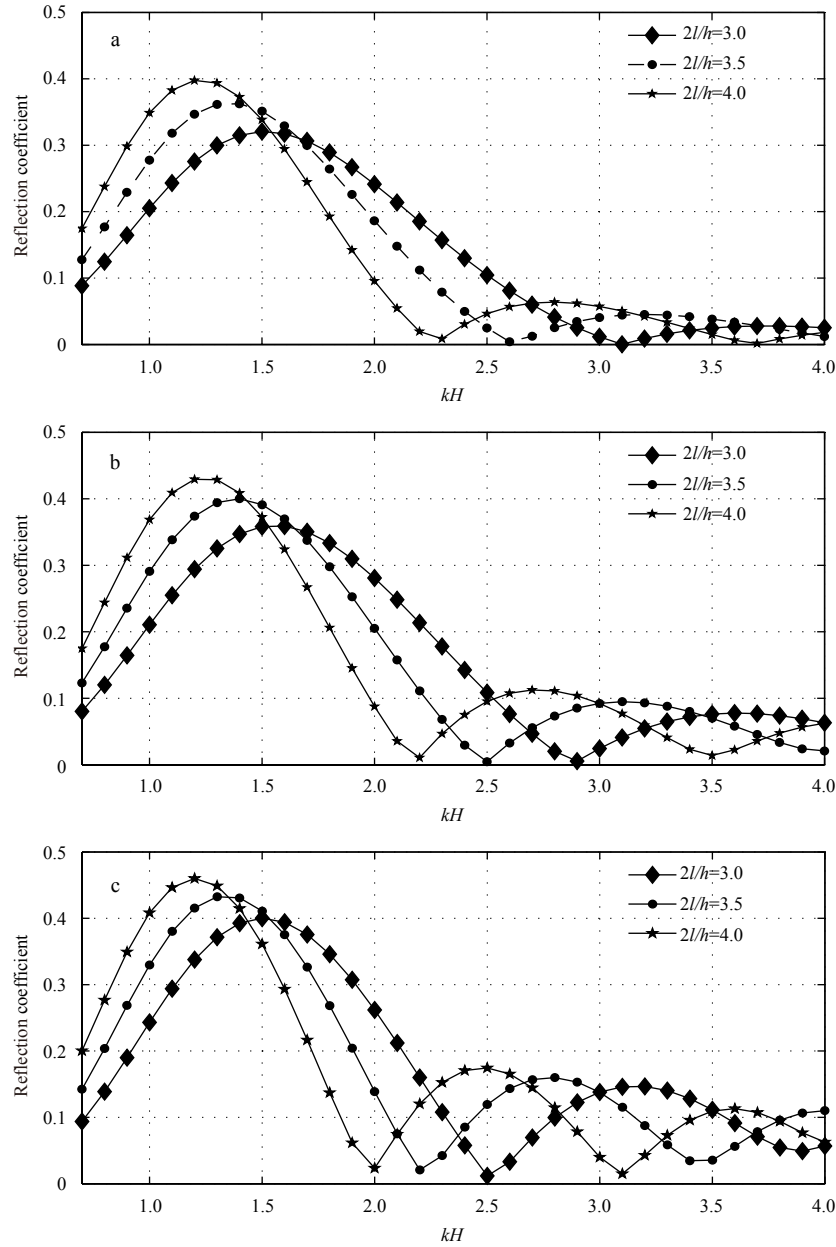
Fig. 10. Reflection coefficient as a function of kH for a thin plate, plate immersion ratio h/H=0.50 and different values of the relative plate length $2l/h$=3.0, 3.5 and 4.0. a. Froud number $U/\sqrt{gH} = 0$, b. $U/\sqrt{gH} = 0.045$, and c. $U/\sqrt{gH}$=0.061.

channel, the relative thickness of the plate, its immersion ratio and its relative length. We studied the effect on the maximum values of the reflection coefficient and the reflection band.

This study was conducted as part of the linearized potential flow theory using the evanescent modes model. To take account of the evanescent modes in the presence of a current, the disper-

sion equation was solved by seeking complex solutions that are neither pure real nor pure imaginary. The number of evanescent modes taken into account was N=30. This investigation revealed that:

(1) Plate thickness influence. The relative plate thickness effect on the reflection coefficient decreases when the immersion

Table 3. Relative difference in the maximum value of the reflection coefficient and reflection bandwidth for different values of the relative plate length ($2l/h$=3, 3.5 and 4) and different values of the Froud number ($U/\sqrt{gH}$=0; 0.045 and 0.061)

$2l/h$	$\dfrac{U}{\sqrt{gH}}=0$			$\dfrac{U}{\sqrt{gH}}=0.045$			$\dfrac{U}{\sqrt{gH}}=0.061$		
	3.0	3.5	4.0	3.0	3.5	4.0	3.0	3.5	4.0
$\left\|\dfrac{M-M_0}{M_0}\right\|$				12%	10.3%	7.8%	24.8%	19.3%	15.7%
$\|k_2H-k_1H\|$	1.02	0.82	0.7	1.00	0.80	0.75	0.85	0.80	0.70

ratio decreases.

(2) Immersion ratio influence. The reflection coefficient maximum and the width of the reflection band decrease with the increase of the plate immersion ratio. When the plate immersion ratio increases, the width of the reflection band is shifted to higher values of kH (short wavelength). When the Froud number increases, the reflection coefficient maximum also increases, and the reflection band is not shifted and is of practically unchanged width.

(3) Plate length influence. The reflection coefficient maximum increases very slightly with the increase of the relative plate length. When the relative plate length increases, the reflection band is shifted to low values of kH (high wavelength), and the width of this band decreases. When the Froud number increases, the reflection coefficient maximum increases as well, and the reflection band is not shifted and is of practically unchanged width.

References

Acanal L, Loukogeorgaki E, Yagci O, et al. 2013. Performance of an inclined thin plate in wave attenuation. Journal of Coastal Research, 1(65): 141–146

Bai Junli, Ma Ning, Gu Xiechong. 2017. Study of interaction between wave-current and the horizontal cylinder located near the free surface. Applied Ocean Research, 67: 44–58, doi: 10.1016/j.apor.2017.06.004

Behera H, Sahoo T. 2015. Hydroelastic analysis of gravity wave interaction with submerged horizontal flexible porous plate. Journal of Fluids and Structures, 54: 643–660, doi: 10.1016/j.jfluidstructs.2015.01.005

Brossard J, Perret G, Blonce L, et al. 2009. Higher harmonics induced by a submerged horizontal plate and a submerged rectangular step in a wave flume. Coastal Engineering, 56(1): 11–22, doi: 10.1016/j.coastaleng.2008.06.002

Errifaiy M, Naasse S, Chahine C. 2016. Analytical determination of the reflection coefficient by the evanescent modes model during the wave-current-horizontal plate interaction. Comptes Rendus Mécanique, 344(7): 479–486, doi: 10.1016/j.crme.2016.03.004

Hsu H H, Wu Y C. 1998. Scattering of water wave by a submerged horizontal plate and a submerged permeable breakwater. Ocean Engineering, 26(4): 325–341, doi: 10.1016/S0029-8018(97)10032-4

Lebon B, Perret G, Coëtmellec S, et al. 2016. A digital holography set-up for 3D vortex flow dynamics. Experiments in Fluids, 57(6): 103, doi: 10.1007/s00348-016-2187-8

Lin Hongxing, Ning Dezhi, Zou Qingping, et al. 2014. Current effects on nonlinear wave scattering by a submerged plate. Journal of Waterway, Port, Coastal, and Ocean Engineering, 140(5): 04014016, doi: 10.1061/(ASCE)WW.1943-5460.0000256

Liu Yong, Li Yucheng, Teng Bin. 2009. Wave motion over two submerged layers of horizontal thick plates. Journal of Hydrodynamics, 21(4): 453–462, doi: 10.1016/S1001-6058(08)60171-7

Liu P L F, Iskandarani M. 1991. Scattering of short-wave groups by submerged horizontal plate. Journal of Waterway, Port, Coastal, and Ocean Engineering, 117(3): 235–246, doi: 10.1061/(ASCE)0733-950X(1991)117:3(235)

Ning Dezhi, Lin Hongxing, Teng Bin, et al. 2014. Higher harmonics induced by waves propagating over a submerged obstacle in the presence of uniform current. China Ocean Engineering, 28(6): 725–738, doi: 10.1007/s13344-014-0057-9

Patarapanich M. 1984. Maximum and zero Reflection from submerged plate. Journal of waterway, Port, Coastal, and Ocean Engineering, 110(2): 171–181, doi: 10.1061/(ASCE)0733-950X(1984)110:2(171)

Patarapanich M, Cheong H F. 1989. Reflection and transmission characteristics of regular and random waves from a submerged horizontal plate. Coastal Engineering, 13(2): 161–182, doi: 10.1016/0378-3839(89)90022-7

Rao S, Shirlal K G, Varghese R V, et al. 2009. Experimental investigation of hydraulic performance of a horizontal plate breakwater. International Journal of Earth Sciences and Engineering, 2: 424–432

Rey V, Capobianco R, Dulou C. 2003. Réflexion de la houle par une plaque immergée en présence d'un courant. Revue de Mécanique Appliquée et Théorique, 1(4): 207–218

Rey V, Touboul J. 2011. Forces and moment on a horizontal plate due to regular and irregular waves in the presence of current. Applied Ocean Research, 33(2): 88–99, doi: 10.1016/j.apor.2011.02.002

Yueh C Y, Chuang S H. 2009. Wave scattering by a submerged porous plate wave absorber. In: Proceedings of the 19th International Offshore and Polar Engineering Conference. Osaka, Japan: International Society of Offshore and Polar Engineers, 1167–1173

Zheng Y H, Liu P F, Shen Y M, et al. 2007b. On the radiation and diffraction of linear water waves by an infinitely long rectangular structure submerged in oblique seas. Ocean Engineering, 34(3–4): 436–450

Zheng Y H, Shen Y M, Tang J. 2007a. Radiation and diffraction of linear water waves by an infinitely long submerged rectangular structure parallel to a vertical wall. Ocean Engineering, 34(1): 69–82, doi: 10.1016/j.oceaneng.2005.12.004

Appendix:

The continuity of the velocity potential at the edge of attack (x=–l):

$$\phi_1\left(-l, y\right) = \phi_3\left(-l, y\right) \quad -h\leqslant y\leqslant 0, \; \phi_1\left(-l, y\right) = \phi_4\left(-l, y\right) \quad -H\leqslant y\leqslant -h. \tag{A1}$$

Multiplying these two equations respectively by $\cos\left(k_{3n}\left(y+h\right)\right)$ and $\cos\left(\mu_n\left(y+H\right)\right)$ and then integrating, we obtain:

$$\int_{-h}^{0}\phi_1\left(-l, y\right)\cos\left(k_{3n}\left(y+h\right)\right)\mathrm{d}y = \int_{-h}^{0}\phi_3\left(-l, y\right)\cos\left(k_{3n}\left(y+h\right)\right)\mathrm{d}y \qquad \left(1\leqslant n\leqslant N\right),$$

$$\int_{-H}^{-h}\phi_1\left(-l, y\right)\cos\left(\mu_n\left(y+H\right)\right)\mathrm{d}y = \int_{-H}^{-h}\phi_4\left(-l, y\right)\cos\left(\mu_n\left(y+H\right)\right)\mathrm{d}y \qquad \left(1\leqslant n\leqslant N\right). \tag{A2}$$

This gives 2N equations (2 equations for each value of n). Two other equations are obtained by replacing $\cos\left(k_{3n}\left(y+h\right)\right)$ by $\cosh\left(k_3\left(y+h\right)\right)$ and $\cos\left(\mu_n\left(y+H\right)\right)$ by 1 (one) in the previous process. Hence, the number of equations is 2N+2.

The continuity of the horizontal velocity at the edge of attack (x=–l):

$$\frac{\partial\phi_1\left(-l, y\right)}{\partial x} = \frac{\partial\phi_3\left(-l, y\right)}{\partial x} \quad -h\leqslant y\leqslant 0, \quad \frac{\partial\phi_1\left(-l, y\right)}{\partial x} = \frac{\partial\phi_4\left(-l, y\right)}{\partial x} \quad -H\leqslant y\leqslant -h. \tag{A3}$$

By multiplying these two equations by $\cos\left(k_{1n}\left(y+H\right)\right)$ and then integrating and summing, we obtain:

$$\int_{-H}^{0}\frac{\partial\phi_1\left(-l, y\right)}{\partial x}\cos\left(k_{1n}\left(y+H\right)\right)\mathrm{d}y = \int_{-h}^{0}\frac{\partial\phi_3\left(-l, y\right)}{\partial x}\cos\left(k_{1n}\left(y+H\right)\right)\mathrm{d}y+$$

$$\int_{-H}^{-h}\frac{\partial\phi_4\left(-l, y\right)}{\partial x}\cos\left(k_{1n}\left(y+H\right)\right)\mathrm{d}y \qquad \left(1\leqslant n\leqslant N\right). \tag{A4}$$

Replacing $\cos\left(k_{1n}\left(y+H\right)\right)$ by $\cosh\left(k_1^+\left(y+H\right)\right)$ in the previous process, we obtain another equation. In addition, by using the matching conditions between the subdomains at the edge of attack, we obtain 3N+3 equations.

Using a similar process at the edge of trailing (x=l), by replacing ϕ_1 by ϕ_2, k_1^+ by k_1^-, $-k_{1n}$ by $-k_{1n}$, k_3^- by k_3^+ and k_{3n} by $-k_{3n}$, we obtain 3N+3 other equations.

Therefore, using the continuity of the velocity potential and of the horizontal velocity at the attack and trailing edges of the plate, we obtain the following system (Eqs (A5)–(A16)):

$$\int_{-h}^{0}\phi_1\left(-l, y\right)\cos\left(k_{3n}\left(y+h\right)\right)\mathrm{d}y = \int_{-h}^{0}\phi_3\left(-l, y\right)\cos\left(k_{3n}\left(y+h\right)\right)\mathrm{d}y \qquad \left(1\leqslant n\leqslant N\right), \tag{A5}$$

$$\int_{-h}^{0}\phi_1\left(-l, y\right)\cosh\left(k_3^-\left(y+h\right)\right)\mathrm{d}y = \int_{-h}^{0}\phi_3\left(-l, y\right)\cosh\left(k_3^-\left(y+h\right)\right)\mathrm{d}y, \tag{A6}$$

$$\int_{-H}^{-h}\phi_1\left(-l, y\right)\cos\left(\mu_n\left(y+H\right)\right)\mathrm{d}y = \int_{-H}^{-h}\phi_4\left(-l, y\right)\cos\left(\mu_n\left(y+H\right)\right)\mathrm{d}y \qquad \left(1\leqslant n\leqslant N\right), \tag{A7}$$

$$\int_{-H}^{-h}\phi_1\left(-l, y\right)\mathrm{d}y = \int_{-H}^{-h}\phi_4\left(-l, y\right)\mathrm{d}y, \tag{A8}$$

$$\int_{-H}^{0}\frac{\partial\phi_1\left(-l, y\right)}{\partial x}\cos\left(k_{1n}\left(y+H\right)\right)\mathrm{d}y = \int_{-h}^{0}\frac{\partial\phi_3\left(-l, y\right)}{\partial x}\cos\left(k_{1n}\left(y+H\right)\right)\mathrm{d}y+$$

$$\int_{-H}^{-h}\frac{\partial\phi_4\left(-l, y\right)}{\partial x}\cos\left(k_{1n}\left(y+H\right)\right)\mathrm{d}y \qquad \left(1\leqslant n\leqslant N\right), \tag{A9}$$

$$\int\limits_{-H}^{0} \frac{\partial \phi_1\left(-l, y\right)}{\partial x} \cosh\left(k_1^+\left(y+H\right)\right) \mathrm{d}y = \int\limits_{-h}^{0} \frac{\partial \phi_3\left(-l, y\right)}{\partial x} \cosh\left(k_1^+\left(y+H\right)\right) \mathrm{d}y +$$
$$\int\limits_{-H}^{-h} \frac{\partial \phi_4\left(-l, y\right)}{\partial x} \cosh\left(k_1^+\left(y+H\right)\right) \mathrm{d}y, \tag{A10}$$

$$\int\limits_{-h}^{0} \phi_2\left(l, y\right) \cos\left(k_{3n}\left(y+h\right)\right) \mathrm{d}y = \int\limits_{-h}^{0} \phi_3\left(l, y\right) \cos\left(k_{3n}\left(y+h\right)\right) \mathrm{d}y \qquad (1 \leqslant n \leqslant N), \tag{A11}$$

$$\int\limits_{-h}^{0} \phi_2\left(l, y\right) \cosh\left(k_3^+\left(y+h\right)\right) \mathrm{d}y = \int\limits_{-h}^{0} \phi_3\left(l, y\right) \cosh\left(k_3^+\left(y+h\right)\right) \mathrm{d}y, \tag{A12}$$

$$\int\limits_{-H}^{-h} \phi_2\left(l, y\right) \cos\left(\mu_n\left(y+H\right)\right) \mathrm{d}y = \int\limits_{-H}^{-h} \phi_4\left(l, y\right) \cos\left(\mu_n\left(y+H\right)\right) \mathrm{d}y \qquad (1 \leqslant n \leqslant N), \tag{A13}$$

$$\int\limits_{-H}^{-h} \phi_2\left(l, y\right) \mathrm{d}y = \int\limits_{-H}^{-h} \phi_4\left(l, y\right) \mathrm{d}y, \tag{A14}$$

$$\int\limits_{-H}^{0} \frac{\partial \phi_2\left(l, y\right)}{\partial x} \cos\left(k_{1n}\left(y+H\right)\right) \mathrm{d}y = \int\limits_{-h}^{0} \frac{\partial \phi_3\left(l, y\right)}{\partial x} \cos\left(k_{1n}\left(y+H\right)\right) \mathrm{d}y +$$
$$\int\limits_{-H}^{-h} \frac{\partial \phi_4\left(l, y\right)}{\partial x} \cos\left(k_{1n}\left(y+H\right)\right) \mathrm{d}y \qquad (1 \leqslant n \leqslant N), \tag{A15}$$

$$\int\limits_{-H}^{0} \frac{\partial \phi_2\left(l, y\right)}{\partial x} \cosh\left(k_1^-\left(y+H\right)\right) \mathrm{d}y = \int\limits_{-h}^{0} \frac{\partial \phi_3\left(l, y\right)}{\partial x} \cosh\left(k_1^-\left(y+H\right)\right) \mathrm{d}y +$$
$$\int\limits_{-H}^{-h} \frac{\partial \phi_4\left(l, y\right)}{\partial x} \cosh\left(k_1^-\left(y+H\right)\right) \mathrm{d}y. \tag{A16}$$

The expressions of potentials Eq. (A1) and Eq. (A4) show that the functions ϕ_p are linear with respect to the constants $\{B_1, B_{1n}, A_3, B_3, A_{3n}, B_{3n}, A_4, B_4, A_{4n}, B_{4n}, A_2$ and A_{2n} for $1 \leqslant n \leqslant N\}$. After integration, Eqs (A5) to (A16) depend on the following constants: the geometrical parameters h/H, $2l/h$ and e/h; the relative depth kH (where k is the wavenumber of the incident wave in the absence of a current); and the Froud number $U/\sqrt{gH}$. As a result, Eqs (A5)–(A16) are also linear with respect to the constants $\{B_1, B_{1n}, A_3, B_3, A_{3n}, B_{3n}, A_4, B_4, A_{4n}, B_{4n}, A_2$ and A_{2n} for $1 \leqslant n \leqslant N\}$. These equations therefore constitute a linear algebraic system of $6N+6$ equations and $6N+6$ unknowns, which are the constants $\{B_1, B_{1n}, A_3, B_3, A_{3n}, B_{3n}, A_4, B_4, A_{4n}, B_{4n}, A_2$ and A_{2n} for $1 \leqslant n \leqslant N\}$. The linearity of this system results from the linearity of the velocity potential. The elements of the matrix corresponding to this system depend on the following: geometrical parameters h/H, $2l/h$ and e/h; the relative depth kH (where k is the wavenumber of the incident wave in the absence of a current); and the Froud number $U/\sqrt{gH}$.